

Nitric oxide-induced calcium release via ryanodine receptors regulates neuronal function

Sho Kakizawa^{1,2,3,8,*}, Toshiko Yamazawa^{1,8}, Yili Chen⁴, Akihiro Ito⁴, Takashi Murayama⁵, Hideto Oyamada⁶, Nagomi Kurebayashi⁵, Osamu Sato⁵, Masahiko Watanabe⁷, Nozomu Mori², Katsuji Oguchi⁶, Takashi Sakurai⁵, Hiroshi Takeshima³, Nobuhito Saito⁴ and Masamitsu Iino^{1,*}

¹Department of Pharmacology, Graduate School of Medicine, The University of Tokyo, Tokyo, Japan, ²Department of Anatomy and Neurobiology, Graduate School of Biomedical Sciences, Nagasaki University, Nagasaki, Japan, ³Department of Biological Chemistry, Kyoto University Graduate School of Pharmaceutical Sciences, Kyoto, Japan, ⁴Department of Neurosurgery, Graduate School of Medicine, The University of Tokyo, Tokyo, Japan, ⁵Department of Pharmacology, Juntendo University School of Medicine, Tokyo, Japan, ⁶Department of Pharmacology, School of Medicine, Showa University, Tokyo, Japan and ⁷Department of Anatomy, Hokkaido University School of Medicine, Sapporo, Japan

Mobilization of intracellular Ca²⁺ stores regulates a multitude of cellular functions, but the role of intracellular Ca²⁺ release via the ryanodine receptor (RyR) in the brain remains incompletely understood. We found that nitric oxide (NO) directly activates RyRs, which induce Ca²⁺ release from intracellular stores of central neurons, and thereby promote prolonged Ca²⁺ signalling in the brain. Reversible S-nitrosylation of type 1 RyR (RyR1) triggers this Ca²⁺ release. NO-induced Ca²⁺ release (NICR) is evoked by type 1 NO synthase-dependent NO production during neural firing, and is essential for cerebellar synaptic plasticity. NO production has also been implicated in pathological conditions including ischaemic brain injury, and our results suggest that NICR is involved in NO-induced neuronal cell death. These findings suggest that NICR via RyR1 plays a regulatory role in the physiological and pathophysiological functions of the brain.

The EMBO Journal (2012) 31, 417–428. doi:10.1038/emboj.2011.386; Published online 28 October 2011

Subject Categories: signal transduction; neuroscience

Keywords: calcium; nitric oxide; ryanodine receptor; synapse

*Corresponding authors. S Kakizawa, Department of Biological Chemistry, Kyoto University Graduate School of Pharmaceutical Sciences, Kyoto 606-8501, Japan. Tel.: +81 75753 4552; Fax: +81 75753 4562; E-mail: sho-kaki@pharm.kyoto-u.ac.jp or M Iino, Department of Pharmacology, Graduate School of Medicine, The University of Tokyo, Tokyo 113-0033, Japan. Tel.: +81 35841 3417; Fax: +81 35841 3390; E-mail: iino@m.u-tokyo.ac.jp

⁸These authors contributed equally to this work

Received: 25 May 2011; accepted: 28 September 2011; published online: 28 October 2011

Introduction

Intracellular Ca²⁺ signalling regulates a myriad of cellular functions (Berridge *et al*, 2000). In addition to Ca²⁺ influx from extracellular spaces, Ca²⁺ is mobilized within the cell from intracellular Ca²⁺ stores through two types of Ca²⁺ release channels: ryanodine receptors (RyRs) and inositol 1,4,5-trisphosphate receptors (IP₃Rs). The opening of RyRs is regulated by Ca²⁺ channels in the plasma membrane. Whereas the opening of type 2 RyR (RyR2) is regulated by an influx of Ca²⁺ via voltage-gated Ca²⁺ channels through the Ca²⁺-induced Ca²⁺ release (CICR) mechanism in cardiac cells, type 1 RyR (RyR1) is physiologically regulated by voltage-gated Ca²⁺ channels through direct protein–protein interactions in skeletal muscle cells (Endo, 2009). Although RyR1 is also expressed in the brain, such tight Ca²⁺ channel-mediated regulation of intracellular Ca²⁺ release via RyR1, as seen in skeletal muscle cells, is absent in central neurons (Kano *et al*, 1995). Therefore, further investigation into the regulatory mechanisms and functions of RyR1 in the brain is warranted.

Nitric oxide (NO) is a ubiquitous intercellular gaseous messenger that is enzymatically generated by NO synthase (NOS) (Bredt and Snyder, 1994). In the brain, NO signalling regulates many physiological and pathophysiological functions, including synaptic plasticity and neuronal cell death. However, the mechanisms by which NO signalling regulates neuronal function require further clarification. *In vitro* single-channel measurements suggest that NO enhances the probability of RyR1 channel opening through S-nitrosylation (Aghdasi *et al*, 1997; Eu *et al*, 2000). This mechanism is implicated in Ca²⁺ leak from skeletal muscle Ca²⁺ stores in pathological conditions (Durham *et al*, 2008; Bellinger *et al*, 2009). However, the functional role of NO-dependent effects on RyR1 in the brain has not yet been elucidated.

Therefore, the objective of the present study was to assess if NO has an effect on RyR1-mediated Ca²⁺ signalling in central neurons. Our findings suggest that NO functions as a RyR1 agonist to release Ca²⁺ from neuronal intracellular Ca²⁺ stores through a reversible S-nitrosylation of the RyR1. The resulting Ca²⁺ signal is required for the induction of NO-dependent synaptic plasticity in the cerebellar synapses. NO generation is associated with many diseases of the brain. Our results suggest that NO-induced Ca²⁺ release (NICR) via RyR1 is involved in neuronal cell death. These findings show a novel form of Ca²⁺ signalling in the brain that plays an important part in health and disease.

Results

NO induces Ca²⁺ release from neuronal intracellular Ca²⁺ stores

We examined potential functional interactions between NO and Ca²⁺ signalling in the cerebellar cortex, where NOS1 is highly expressed in granule cells (Bredt *et al*, 1991). The granule cells extend axons to form glutamatergic synapses on

the dendrites of Purkinje cells (PCs), which abundantly express RyR1 (Furuichi *et al*, 1994). To our surprise, when an NO donor—NOC7 (1-hydroxy-2-oxo-3-(*N*-methyl-3-aminopropyl)-3-methyl-1-triazene) or NOR1 ((\pm)-(*E*)-4-methyl-2-[(*E*)-hydroxyimino]-5-nitro-6-methoxy-3-hexenamide)—was applied to acute cerebellar slices, the intracellular Ca^{2+} concentration ($[\text{Ca}^{2+}]_i$) increased in PC dendrites (Figure 1A and B; Supplementary Figure S1A). The NO-induced Ca^{2+} increase was observed in the absence of extracellular Ca^{2+} (Figure 1D; Supplementary Figure S1B), and was blocked using an inhibitor of the sarco(endo)plasmic reticulum Ca^{2+} ATPase, thapsigargin, which depletes Ca^{2+} stores (Figure 1B and D). These results suggest that NO mediates the release of Ca^{2+} from neuronal intracellular Ca^{2+} stores.

PCs express two types of Ca^{2+} release channels: RyR and IP₃R (Furuichi *et al*, 1994). Of all Ca^{2+} release channel subtypes, RyR1 and IP₃R1 are the most dominant subtypes

expressed in PCs (Furuichi *et al*, 1994; Giannini *et al*, 1995; Wojcikiewicz, 1995; Mori *et al*, 2000; Sawada *et al*, 2008). We examined which of these two channels was responsible for the NO-induced $[\text{Ca}^{2+}]_i$ increase. Application of the IP₃R inhibitor heparin at a concentration (4 mg/ml) sufficient to inhibit IP₃R in PCs (Takechi *et al*, 1998) had no effect on the $[\text{Ca}^{2+}]_i$ increase (Figure 1D; Supplementary Figure S1C). Conversely, a RyR inhibitor, dantrolene, blocked the NO-induced $[\text{Ca}^{2+}]_i$ increase at 36°C (the temperature at which the drug's effects are observed) (Zhao *et al*, 2001) (Figure 1C and D). Thus, RyR1, but not IP₃R, seems to be responsible for the NO-induced $[\text{Ca}^{2+}]_i$ increase. This notion was further examined in mice deficient in RyR1 (Takeshima *et al*, 1994). Because *Ryr1*^{-/-} mice die perinatally, PCs in acute neonatal cerebellar slices were studied. Even though neonatal PCs have poor dendritic arbourization, intracellular Ca^{2+} stores in the somata of *Ryr1*^{+/+} PCs responded to NO

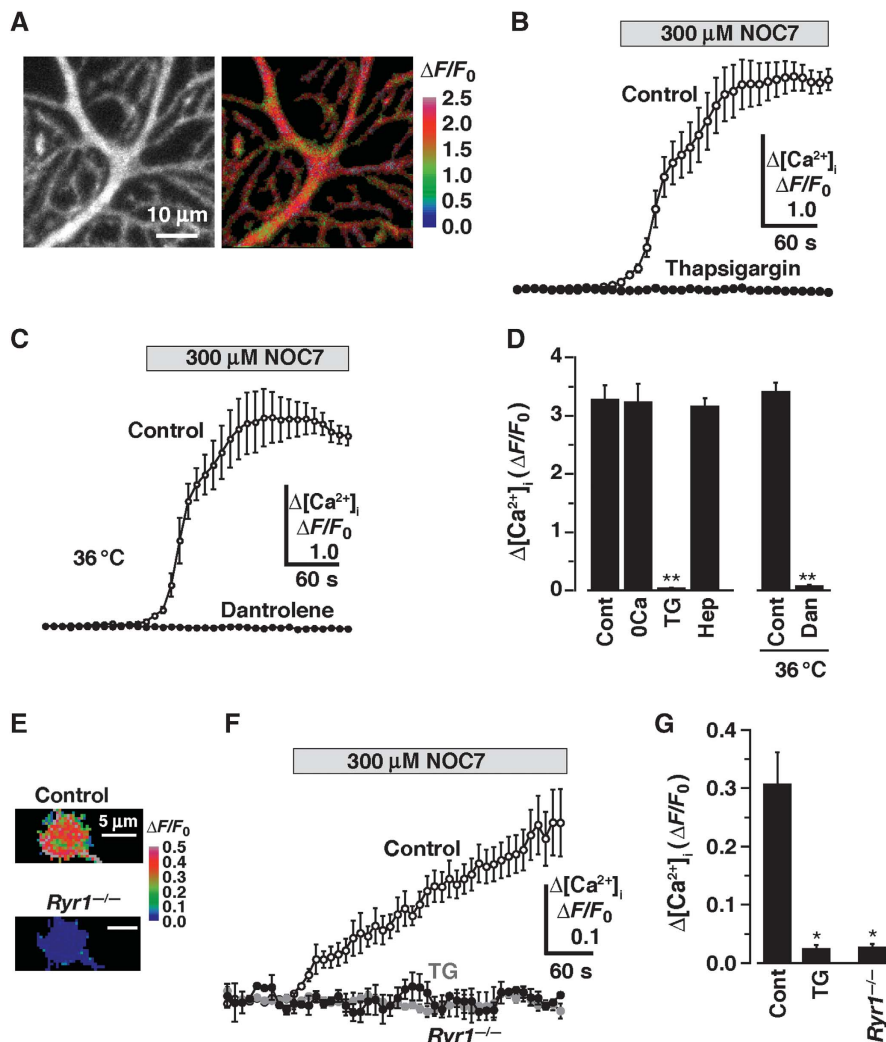


Figure 1 NO induces intracellular Ca^{2+} release via RyR1 in cerebellar PCs. (A) Confocal Ca^{2+} imaging of PC dendrites (left) and pseudocolour Ca^{2+} imaging of cells (right) 120 s following NOC7 (300 μM) treatment. (B) NOC7-induced Ca^{2+} increase with or without thapsigargin (TG) (2 μM). (C) NOC7-induced Ca^{2+} increase at 36°C with or without dantrolene (30 μM). (D) Effect of various perturbations (i.e. removal of extracellular Ca^{2+} with 0.5 mM EGTA (OCa), 2 μM TG, 4 mg/ml heparin applied through a patch pipette (Hep), and 30 μM dantrolene (Dan)) on the peak magnitude of the NO-induced Ca^{2+} response. (E) Confocal Ca^{2+} imaging in the soma of neonatal PCs 120 s after NOC7 (300 μM) treatment in control and *Ryr1*^{-/-} mice. (F) NOC7-induced Ca^{2+} increase in PCs treated with or without TG (2 μM) and in *Ryr1*^{-/-} PCs. (G) Summary of the effect of perturbations on the magnitude of NO-induced Ca^{2+} increase. In all graphs, error bars indicate s.e.m. ($n = 5-11$). * $P < 0.01$, ** $P < 0.001$, *t*-test compared with control.

to release Ca²⁺, and this effect was blocked by thapsigargin and dantrolene (Figure 1E–G; Supplementary Figure S1D). However, NO did not induce Ca²⁺ increase in *Ryr1*^{-/-} PCs (Figure 1E–G). The absence of NO-induced Ca²⁺ responses in *Ryr1*^{-/-} PCs was not due to an impairment of Ca²⁺ stores, because glutamate-induced Ca²⁺ release was observed in the PCs of the mutant mice (Supplementary Figure S1E). These findings indicate that RyR1 underlies the NO-induced [Ca²⁺]_i increase.

NICR in cells expressing exogenous RyR

We then characterized the agonistic effect of NO on RyR1 using HEK293 cells with tetracycline-regulated RyR1 expression (Supplementary Figure S2A and B). In control cells without exogenous RyR1 expression, neither NOC7 nor the RyR agonist, caffeine, induced a change in [Ca²⁺]_i (Supplementary Figure S2C). Conversely, RyR1-expressing cells demonstrated a clear Ca²⁺ response to both NOC7 (Figure 2A and C) and caffeine (Figure 2D) in a dose-dependent manner. This NO-induced Ca²⁺ increase was a reversible process (Supplementary Figure S2D), and this effect was completely blocked by thapsigargin or dantrolene (Figure 2A; Supplementary Figure S2E and F). Taken together, these findings indicate that RyR1 activation is both necessary and sufficient for NO-induced Ca²⁺ release from intracellular stores. This mechanism will be hereafter referred to as 'NICR'.

There are three subtypes of RyR, all of which are expressed in the brain. We examined if subtypes other than RyR1 also function via the NICR mechanism. Cells expressing RyR2 or RyR3 demonstrated a robust response to caffeine (Supplementary Figure S2G). RyR2 has high CICR activity, and cells expressing this subtype generated spontaneous Ca²⁺ oscillations (Supplementary Figure S2G). Despite this, the effect of NO on RyR2 Ca²⁺ release was very slight (Figure 2B; Supplementary Figure S2G). In contrast, cells expressing RyR3 responded to NO, although the sensitivity to NO appeared to be lower than that of RyR1 (Figure 2B; Supplementary Figure S2G). Thus, NICR occurs predominantly via RyR1, to a lesser extent via RyR3, and not via RyR2.

Underlying mechanisms of NICR

NO exerts its effects via two pathways: activation of soluble guanylyl cyclase (sGC) and subsequent cyclic GMP (cGMP) signalling, as well as protein S-nitrosylation (Hess *et al*, 2005). It seems unlikely that NICR occurs via the sGC pathway, as its inhibitor 1*H*-[1,2,4]oxadiazolo[4,3-*a*]quinoxalin-1-one (ODQ) had no inhibitory effects on NICR (Figure 2A; Supplementary Figure S2E). We therefore examined the S-nitrosylation mechanism. RyR1 has several cysteine residues that are susceptible to S-nitrosylation, and S-nitrosylation particularly at cysteine 3635 enhances the open probability of single RyR1 channels in planar bilayers (Moore *et al*, 1999; Sun *et al*, 2001). To examine the role of S-nitrosylation in NICR, we generated HEK293 cells expressing a mutated C3635A-RyR1, where the critical cysteine residue was replaced by alanine (Supplementary Figure S2B). Caffeine, but not NOC7, led to Ca²⁺ release in cells expressing C3635A-RyR1 (Figure 2C and D). Using the biotin-switch method, we then analysed S-nitrosylation of RyR1 (Supplementary Figure S2A). RyR1 was transiently S-nitrosylated by NOC7, but S-nitrosylation was significantly reduced in C3635A-RyR1 (Figure 2E and F). These results indicate that S-nitrosylation of RyR1 is the underlying mechanism of NICR.

We also examined whether cerebellar RyR1 is S-nitrosylated after NOC7 application, and found that RyR1 S-nitrosylation also occurred in cerebellar slice preparations (Supplementary Figure S1F and G).

There was a marked difference in the time course of NOC7-induced Ca²⁺ responses between PCs in slice preparations and HEK293 cells. However, the difference can (at least in part) be accounted for by the lag time in the increase in NOC7 concentration around the neurons, because the NO donor was applied by superfusion of thick slice preparations. In accordance with this notion, the time course of NICR in response to 300 μM NOC7 in cultured cerebral neurons was similar to that of HEK293 cells (Supplementary Figure S1H versus Figure S2G, top left panel).

NICR is induced by neuronal activity

Having shown that exogenous NO induces NICR in RyR1-expressing cells, we then studied whether NICR is evoked by endogenous NO signalling in the brain. When physiologically relevant burst stimulations (BS; five pulses at 50 Hz) (Chadderton *et al*, 2004) are repeatedly applied, parallel fibres (PFs) generate local NO signals near the PF-PC synapses that reach micromolar concentrations in acute cerebellar slices (Namiki *et al*, 2005). Thus, we assessed [Ca²⁺]_i in PC dendrites receiving intrinsic NO signalling from PFs. Stimulus intensity was adjusted to ensure that glutamatergic Ca²⁺ responses to a single BS were negligible in postsynaptic PC dendrites (Supplementary Figure S3A). A gradual increase in Ca²⁺ was observed in PC dendrites after repetitive application of BS to PFs at 1 Hz for 60 s (Figure 3A–C), and [Ca²⁺]_i slowly decreased after termination of BS (Figure 3C). The magnitude of the BS-induced Ca²⁺ response was comparable with that of the glutamatergic response observed with a high-frequency PF input, but the time course of the BS response was much slower (Supplementary Figure S3B versus C). The BS-induced Ca²⁺ signal was localized on the dendrites near the stimulation electrode (Figure 3A and B), similar to the PF-derived NO signal (Namiki *et al*, 2005). Depletion of Ca²⁺ stores by thapsigargin abolished the Ca²⁺ increase (Figure 3C and E). Treatment with the IP₃R inhibitor heparin via a patch pipette had no effect on the BS-induced Ca²⁺ increase (Figure 3E; Supplementary Figure S3D), even though the concentration of heparin (4 mg/ml) used was sufficient to inhibit metabotropic glutamate receptor (mGluR)-mediated, IP₃-dependent Ca²⁺ release in PCs (Supplementary Figure S3B). The inhibitory effect of heparin on IP₃-dependent Ca²⁺ release was corroborated by another report (Takechi *et al*, 1998). Conversely, BS-induced Ca²⁺ signalling was blocked by dantrolene (Figure 3D and E). These results indicate that the BS-induced slow [Ca²⁺]_i increase is dependent on Ca²⁺ release via RyR. Glutamatergic signalling is unlikely to be involved, because the BS-induced Ca²⁺ release was observed in the presence of both ionotropic and mGluR antagonists, NBQX (2,3-dioxo-6-nitro-1,2,3,4-tetrahydrobenzo[*f*]quinoxaline-7-sulfonamide) and CPCCOEt (7-(hydroxyimino)cyclopropa[*b*]chromen-1α-carboxylate ethyl ester), respectively (Figure 3E; Supplementary Figure S3G). We confirmed that these glutamate receptor antagonists inhibit glutamatergic Ca²⁺ responses in PCs (Supplementary Figure S3B). Furthermore, an NMDA receptor inhibitor, AP5 (D-(–)-2-amino-5-phosphonopentanoic acid), did not have any effect on the BS-induced Ca²⁺ release (Supplementary Figure S3H).

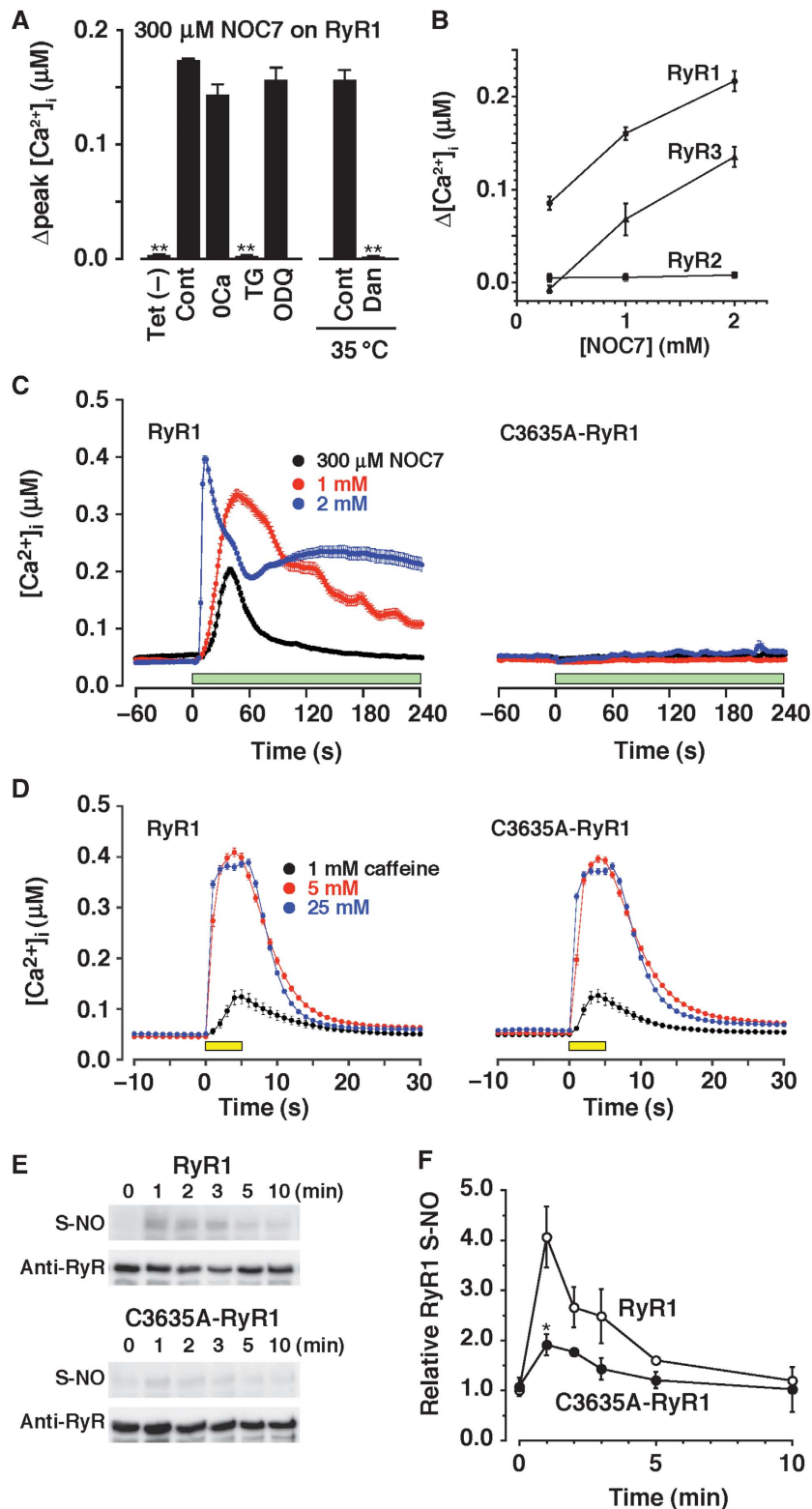


Figure 2 NICR in HEK293 cells expressing RyR1. (A) Effect of various perturbations (i.e. without tetracycline induction, control, removal of extracellular Ca^{2+} with 1 mM EGTA (0Ca), 2 μM thapsigargin (TG), 1 μM ODQ, control at 35 °C and 30 μM dantrolene) on the peak magnitude of NOC7 (300 μM)-induced Ca^{2+} increase; $n = 50$ –145. (B) RyR subtype dependence of the NO-induced Ca^{2+} response. Please refer to Supplementary Figure S2G for more information. (C, D) Ca^{2+} response to NOC7 and caffeine in HEK293 cells expressing RyR1 (left) or C3635A-RyR1 (right); $n = 121$ –245. (E) Time course of NOC7 (1 mM)-induced S-nitrosylation of wild-type and C3635A-RyR1 cells, as determined by the biotin-switch method. (F) Summary of the time course of S-nitrosylation; $n = 3$ –4. In all graphs, error bars indicate s.e.m. * $P < 0.02$, ** $P < 0.001$, *t*-test compared with control.

We also examined if NO is causally involved in the BS-induced Ca^{2+} release. We found that the NOS inhibitor, L-NAME (N^G -Nitro-L-arginine methyl ester), completely

blocked the BS-induced Ca^{2+} release (Figure 3E; Supplementary Figure S3I). We also studied mutant mice deficient in NOS1 (Huang *et al*, 1993). The BS-induced NO signal

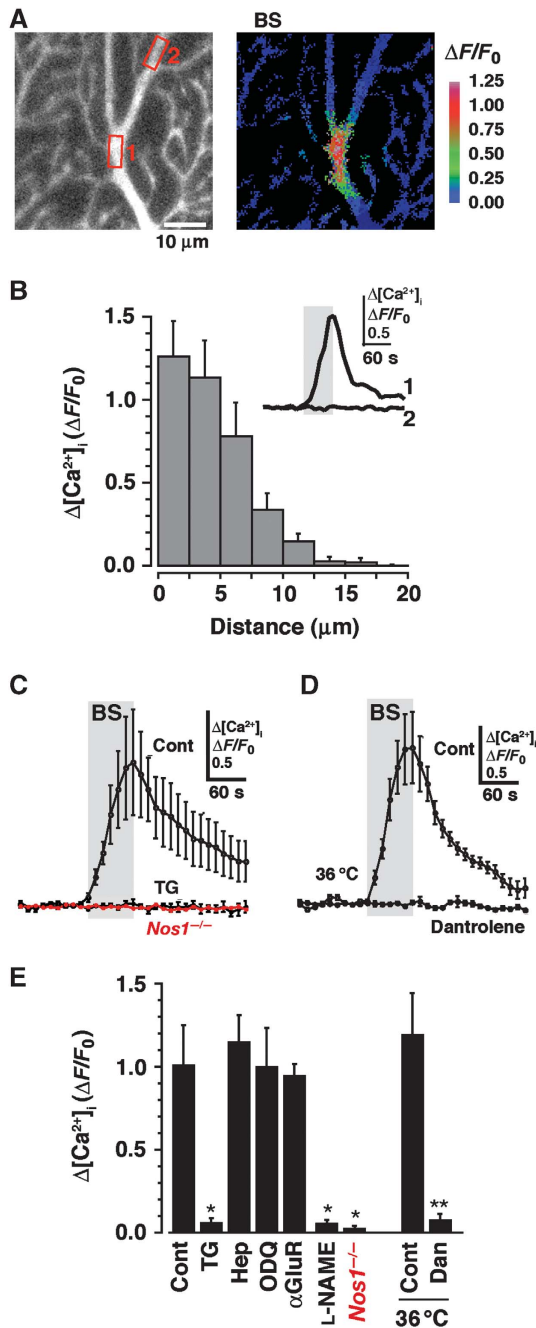


Figure 3 Nerve activity induces NICR in PCs. (A) Confocal Ca^{2+} imaging of PC dendrites (left) and pseudocolour Ca^{2+} imaging of cells (right) 60 s after BS (five pulses at 50 Hz repeated 60 times every 1 s). (B) Spatial distribution of BS-induced Ca^{2+} release; $n = 5$. (C) BS-induced Ca^{2+} increase in wild-type and $\text{Nos1}^{-/-}$ mice with or without thapsigargin (2 μM); $n = 5-6$. (D) BS-induced Ca^{2+} increase in wild-type mice with or without dantrolene (30 μM) at 36°C; $n = 5-6$. (E) Effect of various perturbations on the magnitude of BS-induced Ca^{2+} increase. Control, thapsigargin, heparin (4 mg/ml) applied through a patch pipette, ODQ (1 μM), cocktail of glutamate receptor antagonists (αGluR : 20 μM NBQX and 100 μM CPCCOEt), L-NAME (100 μM), $\text{Nos1}^{-/-}$, control at 36°C, and dantrolene, $n = 5-7$. In all graphs, error bars indicate s.e.m. * $P < 0.01$, ** $P < 0.001$, t -test compared with control.

PF stimulation (Supplementary Figure S3M). Additionally, there was no $[\text{Ca}^{2+}]_i$ increase in response to BS in the PCs of $\text{Nos1}^{-/-}$ mice (Figure 3C and E), even though an exogenous NO source, NOC7 (30 and 300 μM), induced a significant $[\text{Ca}^{2+}]_i$ increase, which is comparable with that in $\text{Nos1}^{+/+}$ mice (Supplementary Figure S3P). Thus, BS-induced Ca^{2+} release is dependent on NOS1-induced NO generation. ODQ (1 and 10 μM) had no inhibitory effects on BS-induced Ca^{2+} release (Figure 3E; Supplementary Figure S3E and F). In addition, ascorbic acid (which has been used for selective reduction of cysteine S -nitrosothiols (Jaffrey *et al*, 2001; Burgoyne and Eaton, 2010)) applied to PCs through the patch pipette abolished BS-induced Ca^{2+} release (Supplementary Figure S3J). These findings are consistent with the involvement of S -nitrosylation, rather than sGC-cGMP signalling, in BS-induced Ca^{2+} release. Furthermore, there were no significant changes in the BS-induced Ca^{2+} release in $\text{Ryr3}^{-/-}$ mice (Supplementary Figure S3K). Taken together, these findings indicate that PFs stimulated in a physiological manner generate NO, which in turn induces NICR via RyR1 in PCs.

Critical role of NICR in cerebellar long-term potentiation

We next studied the potential physiological or pathophysiological roles of NICR. BS-induced NO generation by PFs also induces long-term potentiation (LTP) in the PF-PC synapse (Namiki *et al*, 2005). This form of LTP is similar to PF-LTP, generated by PF stimulation at 1 Hz for 5 min (Lev-Ram *et al*, 2002; Coesmans *et al*, 2004), in that both are generated postsynaptically and are NO dependent, although they are not cGMP dependent. PF-LTP is dependent upon the level of $[\text{Ca}^{2+}]_i$ in PC dendrites (Coesmans *et al*, 2004). Confirming that PF stimulation at 1 Hz for 5 min induces LTP (Supplementary Figure S4K), we measured $[\text{Ca}^{2+}]_i$ in PC dendrites during PF stimulation at 1 Hz. We observed an increase in $[\text{Ca}^{2+}]_i$ with a peak amplitude comparable with that during BS stimulation (Supplementary Figure S3L). Consideration of these previous findings and our findings suggests that NICR may be involved in synaptic plasticity, and we tested this possibility.

Repeated BS (60 times at 1 Hz) applied to PFs induced a significant potentiation in PF-PC synapses that lasted > 30 min (Figure 4A). This LTP was absent in $\text{Nos1}^{-/-}$ mice (Figure 4A and C), although LTP in the $\text{Nos1}^{-/-}$ cerebellum could be induced by NOC7 as in wild-type animals (Supplementary Figure S4L). Furthermore, ODQ (10 μM) had no inhibitory effect (Supplementary Figure S4G), although 1 μM of ODQ was sufficient to inhibit long-term depression (LTD) in the same synapse of the cerebellar slice preparations (Supplementary Figure S4M and N), which is known to be dependent upon cGMP signalling (Ito, 2002). These results confirm that BS-induced LTP is NO dependent but not cGMP dependent. Consistent with the central role of NO in LTP induction, mGluR or NMDA receptor blockade did not have a significant effect on LTP (Figure 4C; Supplementary Figure S4E and F). We then tested if intracellular Ca^{2+} release has a role in the induction of LTP. Indeed, depletion of intracellular Ca^{2+} stores by thapsigargin abolished LTP (Figure 4C; Supplementary Figure S4B and L). Furthermore, dantrolene applied in the bath or intracellularly to PCs through a patch pipette blocked LTP (Figure 4B and C; Supplementary Figure S4C), whereas intracellular application

in PCs measured using a NO probe (HBR-GFP) (Namiki *et al*, 2005) was found to be absent in $\text{Nos1}^{-/-}$ mice, indicating that NOS1 is the dominant source of NO upon

of heparin to PCs had no significant effect (Figure 4C; Supplementary Figure S4D). These findings indicate that Ca^{2+} release via RyR, but not IP_3R , is required for the induction of LTP. We also found that the *S*-nitrosylation decomposer ascorbic acid blocked LTP (Supplementary Figure S4H). Although the dominant RyR subtype in PCs is RyR1, RyR3 is also expressed. However, cerebellar LTP was similarly induced in slice preparations of *Ryr3*^{-/-} mice (Supplementary Figure S4I). Intracellular application of a Ca^{2+} buffer, BAPTA (5–30 mM), to PCs through a patch pipette inhibited LTP in a concentration-dependent manner (Figure 4C; Supplementary Figure S4J). Although LTP was observed in the presence of 5 mM BAPTA, 10 mM BAPTA was sufficient to inhibit LTP. The concentration-dependent effect of BAPTA on LTP suggests that local Ca^{2+} signalling rather than a global increase in the dendritic $[\text{Ca}^{2+}]_i$ is required for LTP induction (see Discussion). Taken together, these findings indicate that NICR via the RyR1 in PCs is essential for inducing LTP in PF-PC synapses of the cerebellum.

Involvement of NICR in neuronal cell death

Cerebral ischaemia causes NOS-dependent NO generation. NOS1-dependent NO generation is implicated in ischaemic brain injury, whereas NO generation by type 3 (or endothelial) NOS is considered beneficial to brain injury because it

increases blood flow (Iadecola, 1997). Indeed, brain injury after middle cerebral artery occlusion (MCAO) is significantly milder in mice treated with a NOS1-specific inhibitor and in *Nos1*^{-/-} mice (Huang *et al*, 1994). The NO concentration reaches micromolar levels in ischaemic cerebral tissue during and after MCAO (Malinski *et al*, 1993). Such NO signalling during ischaemia is expected to activate NICR in neurons. We therefore examined whether or not NICR is involved in NOS1-dependent brain injury.

We first used a mouse MCAO model to examine the potential role of NICR in ischaemic brain injury. In line with another study (Huang *et al*, 1994), ischaemic brain injury in the MCAO model was milder in *Nos1*^{-/-} mice than in *Nos1*^{+/+} mice (Figure 5A and B). We then examined the effects of the NICR inhibitor dantrolene, and found that subarachnoidal administration of dantrolene after reperfusion of MCAO had a protective effect on MCAO-induced brain injury in *Nos1*^{+/+} mice (Figure 5A and B). These findings are corroborated by similar findings in other animal models (Li *et al*, 2005). Conversely, there was very little effect of dantrolene on infarction volume in *Nos1*^{-/-} mice (Figure 5B). These results suggest that NOS1-dependent NICR may play a role in ischaemic brain injury following reperfusion in the MCAO model.

We next analysed the potential role of NICR in NO-induced neuronal cell death in culture. NOC12 (a sister NO donor with

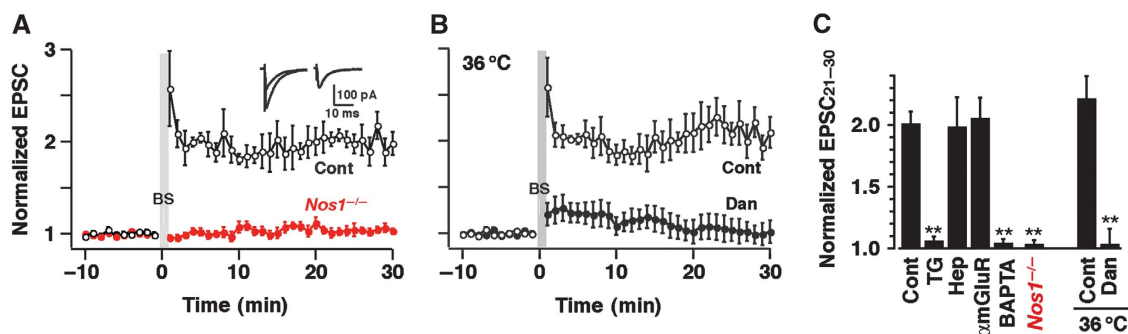


Figure 4 Involvement of NICR in synaptic plasticity. (A) LTP of excitatory postsynaptic currents (EPSCs) at the PF-PC synapse in wild-type and *Nos1*^{-/-} mice; *n* = 5. (B) Dantrolene (30 μM) blocked PF-LTP at 36°C; *n* = 5–6. (C) Effect of various perturbations on the magnitude of LTP (normalized EPSC averaged between 21 and 30 min after BS): control, thapsigargin (2 μM), heparin (4 mg/ml) applied through a patch pipette, CPCCOEt (100 μM, αmGluR), BAPTA (30 mM) applied through a patch pipette, control at 36°C, dantrolene (30 μM), and *Nos1*^{-/-}; *n* = 4–6. ***P* < 0.001, *t*-test compared with control.

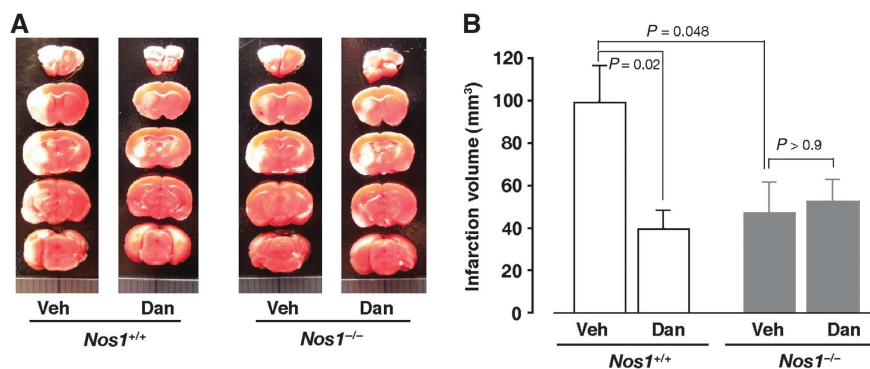


Figure 5 Possible involvement of NICR in ischaemic brain damage. (A) Representative TTC-stained brain slices 24 h after transient MCAO. (B) Infarct volume 24 h after transient MCAO determined using the Leach correction; *n* = 6 for each condition. A two-way ANOVA revealed a significant interaction (*P* = 0.026), and subsequent analyses with Tukey's multiple comparison test indicated that *Nos1*^{+/+} mice treated with dantrolene had a significantly smaller infarct volume compared with *Nos1*^{-/-} mice. Data are the mean ± s.e.m. Physiological data of the animals are summarized in Supplementary Table S1.

a longer half-life than NOC7) was used to mimic a prolonged increase in NO concentrations during brain ischaemia (Malinski *et al*, 1993) (see Supplementary data). NOC12 induced an increase in [Ca²⁺]_i in cerebral neurons of wild-type mice (Figure 6A, left). The [Ca²⁺]_i increase was observed in the absence of extracellular Ca²⁺, and was abolished in the presence of dantrolene (Figure 6B) or in cerebral neurons from *Ryr1*^{-/-} mice (Figure 6A, right). We thus confirmed the presence of NICR in cerebral neurons. When we examined neuronal cell death after application of NOC12, there was a significant increase in cerebral neuron death 16 h after the NO donor treatment (Figure 6C and D). However, in the presence of dantrolene, NO donor-induced neuronal cell death was significantly attenuated (Figure 6C and D). These results suggest that NICR is (at least in part) involved in NO-induced neuronal cell death. Dantrolene may have effects other than NICR inhibition, so we further studied the role of NICR in neuronal cell death using cerebral neurons

obtained from *Ryr1*^{-/-} mice (Figure 6A, right). Consistent with the notion that NICR is involved in NO-induced cell death, cell death was significantly lower in *Ryr1*^{-/-} neurons compared with *Ryr1*^{+/+} neurons (Figure 6C and D). In addition, dantrolene had no protective effect on NO donor-induced cell death in *Ryr1*^{-/-} neurons (Figure 6C and D). Taken together, these findings suggest that NICR via RyR1 contributes to NO-induced neuronal cell death.

The potential importance of S-nitrosylation of RyR1 in NO-induced cell death was examined in HEK cells expressing extrinsic RyR1. NOC12 application induced a dose-dependent increase in [Ca²⁺]_i in cells expressing RyR1, but not in cells expressing C3635A-RyR1 (Supplementary Figure S5A), as in the case of NOC7 (Figure 2C). The NOC12-induced Ca²⁺ increase was abolished by 10 μM dantrolene (Supplementary Figure S5B). We then analysed the effect of NOC12 on cell viability using the MTT assay 16 h after the NO donor treatment. NOC12 induced dose-dependent suppression

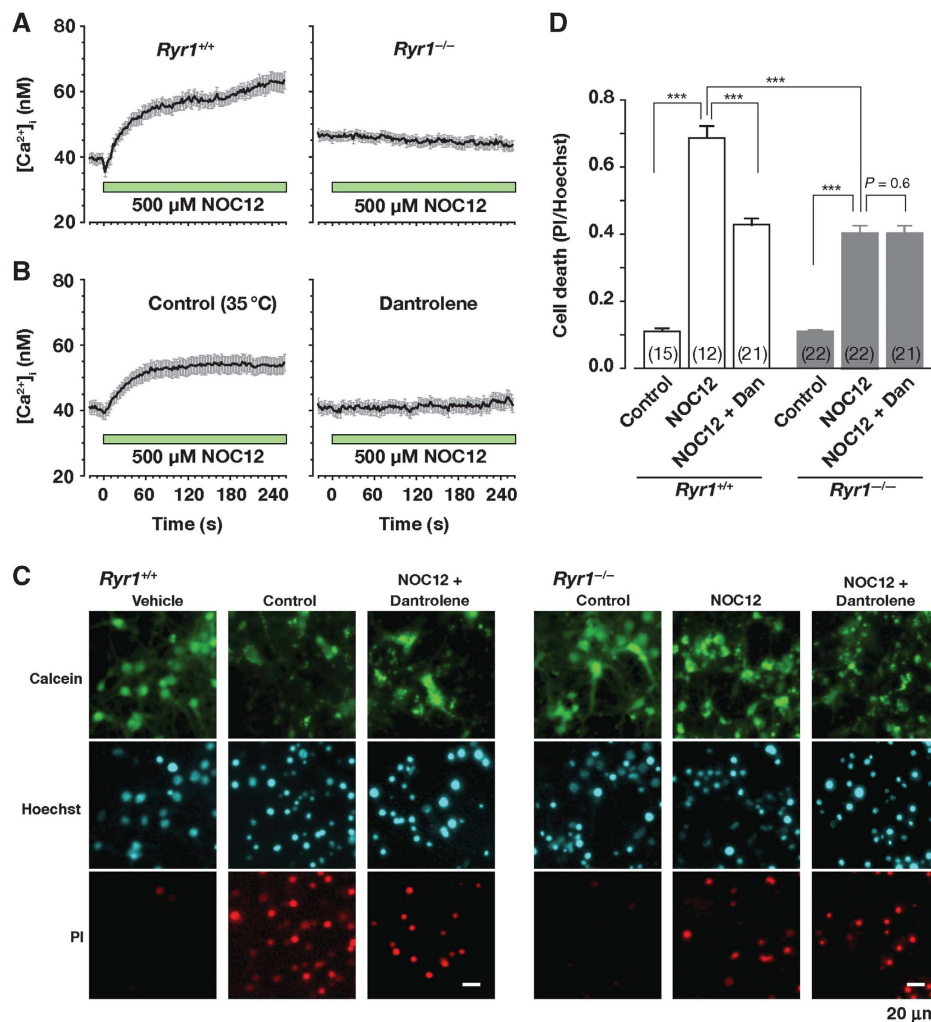


Figure 6 Involvement of NICR in NO-induced neuronal cell death. (A) NOC12 (500 μM)-induced intracellular Ca²⁺ increase in cultured cerebral neurons of *Ryr1*^{+/+} (left, *n* = 30 cells) or *Ryr1*^{-/-} (right, *n* = 28 cells) mice. Ca²⁺ measurements were made in the absence of extracellular Ca²⁺. (B) NOC12-induced Ca²⁺ release is blocked by dantrolene (10 μM) at 35°C. Control, *n* = 22 cells; dantrolene, *n* = 21 cells. (C) Neuronal cell death assayed 16 h after treatment with 500 μM NOC12 without or with 10 μM dantrolene in cultured cerebral neurons of *Ryr1*^{+/+} (left) or *Ryr1*^{-/-} (right) mice. (D) The extent of cell death was expressed as a ratio of the number of PI-positive cells to that of Hoechst-positive cells. Numbers in parentheses (15–22) indicate the number of determinations in each condition using different cultures. In each determination, > 120 cells were analysed. Data are expressed as mean ± s.e.m. Statistical significance was determined via an ANOVA followed by a Tukey *post-hoc* test. ****P* < 0.0001.

of cell viability in cells expressing wild-type RyR1 (Supplementary Figure S5C). Although the same effect of anisomycin on cell viability was observed in cells expressing RyR1 or C3635A-RyR1, the effect of NOC12 was significantly attenuated in cells expressing C3635A-RyR1 at 2 and 3 mM NOC12, but not at 1 mM NOC12, where Ca^{2+} release was not observed (Supplementary Figure S5A). Furthermore, dantrolene, which blocks NOC12-induced Ca^{2+} increase (Supplementary Figure S5B), showed a protective effect against 3 mM NOC12-induced cell viability loss in cells expressing wild-type RyR1, but not in cells expressing C3635A-RyR1 (Supplementary Figure S5C). These results support the notion that S-nitrosylation-dependent NICR is one of the regulators of cell viability.

Discussion

In the present study, it was found that NO induces Ca^{2+} release via RyR1 in central neurons. The agonistic effect of NO on intracellular Ca^{2+} release is mediated by S-nitrosylation of RyR1, in particular at cysteine 3635 of the Ca^{2+} release channel in an extrinsic expression system. The same mechanism may underlie the NO-induced Ca^{2+} responses in neurons, although confirmation is required. The modulation of Ca^{2+} release via S-nitrosylation of RyR1 has been implicated in skeletal muscle contractions in low PO_2 and pathological conditions (Eu *et al*, 2003; Durham *et al*, 2008; Bellinger *et al*, 2009). Thus, although RyR1 is primarily regulated by voltage-gated Ca^{2+} channels through direct protein-protein interactions in skeletal muscle cells, NO-induced S-nitrosylation of RyR1 has a modulatory, enhancing effect on Ca^{2+} release in these cells. However, the tight regulation of RyR1 via Ca^{2+} channels, as seen in skeletal muscle cells, has not yet been demonstrated in central neurons (Kano *et al*, 1995). In contrast to the rapid and transient RyR1-mediated Ca^{2+} release events as seen during twitch and tetanus contractions in skeletal muscle, NICR induced by synaptic input in central neurons produces a much slower and prolonged increase in $[\text{Ca}^{2+}]_i$. It remains to be elucidated if NO has a similar direct Ca^{2+} -releasing effect via RyR1 outside the brain, where the time course of NICR can be influenced by many factors. These include the expression levels of RyR1 and SERCA, the time course of NO increase and the rate of removal of S-nitrosylation.

Other subtypes of RyR, RyR2 and RyR3 are also expressed in the brain. It was found that RyR3 also mediates NICR. RyR1 is the most dominant RyR subtype found in cerebellar PCs (Furuichi *et al*, 1994; Giannini *et al*, 1995; Mori *et al*, 2000; Sawada *et al*, 2008), and it is likely that this subtype mediates NICR and LTP in these cells. Supporting this notion, PCs of *Ryr3*^{-/-} mice demonstrated BS-induced NICR and LTP, whose levels were comparable with that of wild-type mice (Supplementary Figures S3K and S4I). Despite this, it remains to be examined whether NICR via RyR3 has physiological and pathophysiological roles in other regions of the brain.

Unlike RyR1 in skeletal muscle, RyR2 is regulated by the CICR mechanism in cardiac muscle. Corroborating the results of another report (Sun *et al*, 2008), there was virtually no direct effect of NO on Ca^{2+} release via RyR2 (Figure 2B). Given that the important cysteine residue (i.e. cysteine 3635 of RyR1) is conserved among all RyR subtypes (Supplementary Figure S2H), subtype specificity in NICR is

remarkable. Thus, the three-dimensional structure around the critical cysteine residue may be important for S-nitrosylation or channel gating. However, this mechanism requires further clarification. Interestingly, RyR2 can be activated by S-nitrosoglutathione, which can also be formed in the brain (Kluge *et al*, 1997; Sun *et al*, 2008). Dantrolene, which does not block RyR2 (Zhao *et al*, 2001), abolished NICR and LTP in PCs, so S-nitrosoglutathione-mediated RyR2 activation is not likely to play a major part in the neuronal functions explored in the present study.

NICR is induced by mimicking physiological patterns of neuronal activity, and is essential in inducing cerebellar LTP, which is the reverse process of cerebellar LTD (Lev-Ram *et al*, 2003; Coesmans *et al*, 2004). Cerebellar LTP has also been implicated in the memory of fear (Sacchetti *et al*, 2004). As to the molecular mechanism of LTP, N-ethylmaleimide-sensitive factor (NSF)-dependent recruitment of AMPAR in the post-synaptic membrane has been shown to underlie cerebellar LTP (Kakegawa and Yuzaki, 2005). Furthermore, S-nitrosylation of NSF promotes the surface expression of AMPA receptors in central neurons (Huang *et al*, 2005). These previous results indicate that NSF is an important target of NO in cerebellar LTP induction. Cerebellar LTP depends not only on NO but also on the level of $[\text{Ca}^{2+}]_i$ in PCs (Coesmans *et al*, 2004). However, the relationship between these signals is incompletely understood. NICR is a plausible candidate that links NO and $[\text{Ca}^{2+}]_i$. In general agreement with this notion, intracellular application of BAPTA (5–30 mM) to PCs had a dose-dependent inhibitory effect on LTP (Supplementary Figure S4J). Interestingly, 5 mM BAPTA was not sufficient to inhibit LTP, in line with the successful generation of 1 Hz-LTP in the presence of 5 mM BAPTA (Lev-Ram *et al*, 1995). The absence of an inhibitory effect of 5 mM BAPTA on LTP may be partly explained by prevention of residual LTD (Lev-Ram *et al*, 1995). Because 5 mM BAPTA is expected to inhibit a global increase in the dendritic $[\text{Ca}^{2+}]_i$, the result may also suggest involvement of local Ca^{2+} signalling in the generation of LTP. Single-channel openings of RyR1 and RyR2 generate ionic currents of ~ 0.5 pA under near-physiological ionic conditions (Kettlun *et al*, 2003). These unitary events would generate a localized increase in $[\text{Ca}^{2+}]_i$ around the RyR. A recent study showed that the Ca^{2+} -binding rate constants of calmodulin are so high that calmodulin can effectively 'trap' Ca^{2+} immediately when Ca^{2+} enters the cytoplasm before it binds to cytoplasmic Ca^{2+} buffers (Faas *et al*, 2011). Therefore, if calmodulin or other Ca^{2+} -binding proteins with similar Ca^{2+} -binding properties are involved in the signalling process downstream of the Ca^{2+} release from the RyR, it is possible that lower concentrations of BAPTA cannot completely block the process. An example can be found in cardiac cells, in which RyR2 and L-type Ca^{2+} channels localize closely together at the junction between the sarcoplasmic reticulum and plasma membrane. L-type Ca^{2+} channels undergo inactivation in response to an increase in $[\text{Ca}^{2+}]_i$ through a calmodulin-dependent mechanism (Peterson *et al*, 1999; Zühlke *et al*, 1999). Ca^{2+} release from RyR2 facilitates the Ca^{2+} -dependent inactivation of L-type Ca^{2+} channels, and the extent of facilitation is suppressed by intracellular application of BAPTA (3 and 10 mM) in a concentration-dependent manner. However, a considerable fraction of Ca^{2+} release-dependent inactivation remains even in the presence of BAPTA: about 61 and 32% of control

with 3 and 10 mM BAPTA, respectively, at -20 mV (Sham, 1997). Under this experimental condition, RyR2 is activated by Ca^{2+} influx through L-type Ca^{2+} channels, so BAPTA also inhibits the activation of RyR2 itself. Therefore, the inhibitory effect of BAPTA on Ca^{2+} release-induced L-type Ca^{2+} channel inactivation *per se* is overestimated. These considerations suggest that close localization of RyR1 and downstream signal transduction molecules may be involved in the generation of LTP. Of course, this mechanism requires further clarification. Taken together, RyR1 is very likely to be another essential target of NO in cerebellar LTP induction. NOS1 and RyR1 are co-expressed in various regions of the brain, so NICR may have additional physiological roles in the brain.

NO is implicated in various pathological conditions, including ischaemic brain injury, via the generation of reactive nitrogen species such as peroxynitrite (Pacher *et al*, 2007). Our results suggest that NICR via RyR1 is also involved in NO-induced cell death in cerebral neurons in culture. The NO-induced neuronal cell death was significantly milder in *RyR1*^{-/-} neurons, in which NICR was absent. In addition, the NO-induced neuronal cell death was attenuated by dantrolene (which inhibits NICR), and the protective effect of dantrolene was absent in *Ryr1*^{-/-} neurons. Dantrolene also had a protective effect on ischaemic brain injury in the MCAO model. Taken together, these findings suggest that NOS1-dependent NO generation may exert its adverse effects in ischaemic neuronal cell death, in part, via NICR, causing either an excessive increase in neuronal Ca^{2+} concentrations or depleting intracellular Ca^{2+} stores, which in turn stresses the endoplasmic reticulum (Li *et al*, 2005). We studied the importance of cysteine 3635 of RyR1 in cell viability in HEK293 cells. The results suggested that the cysteine residue is one of the important factors in NO-induced cell death. To corroborate the notion of the involvement of NICR in ischaemic neuronal cell death, we tried to measure S-nitrosylation levels of RyR1 in the cerebral cortex. Thus far, the measurement has been difficult because the level of protein expression of RyR1 in the mouse cerebral cortex is not sufficiently high for reliable determination with the biotinswitch method. A new detection method with a higher sensitivity is needed, and this issue should be addressed in future studies. Ischaemic brain injury is a complex process, and the roles of NICR in the disease process require further clarification. With this reservation, it seems possible that drugs that inhibit NICR may have therapeutic value in some forms of ischaemic brain injury.

Materials and methods

Experiments using animals

All animal-related procedures were in accordance with the guidelines of The University of Tokyo (Tokyo, Japan).

Slice preparation and whole-cell patch-clamp recording

C57BL/6 mice (postnatal days 24–32) were sacrificed by cervical dislocation under anaesthesia with diethyl ether. The cerebellum was excised, and parasagittal cerebellar slices (250- μm thick) were prepared from the vermis (Edwards *et al*, 1989; Kakizawa *et al*, 2000, 2005). *Nos1*^{-/-} and *Nos1*^{+/-} mice (Huang *et al*, 1993) were obtained from The Jackson Laboratory. In experiments using *Ryr1*^{-/-} mice, cerebellar slices were prepared from neonatal animals because of the neonatal lethality of these mice (Takeshima *et al*, 1994). *Ryr3*^{-/-} mice were also used (Takeshima *et al*, 1996). Whole-cell recordings were obtained from visually identified PCs under an upright microscope (BX51WI; Olympus, Tokyo, Japan)

using a $\times 40$ water-immersion objective at room temperature (23 – 25°C), with the exception of experiments that used dantrolene ($36 \pm 1^\circ\text{C}$). The resistance of the patch pipettes was 2.0 – 3.5 M Ω when filled with an intracellular solution (in mM) composed of 130 K-gluconate, 10 KCl, 10 NaCl, 4 ATP-Mg, 0.4 GTP-Na and 10 HEPES (pH 7.3; adjusted with KOH). The standard bathing solution (in mM) was composed of 125 NaCl, 2.5 KCl, 2 CaCl_2 , 1 MgSO_4 , 1.25 NaH_2PO_4 , 26 NaHCO_3 and 20 glucose, bubbled with 95% CO_2 and 5% CO_2 . Bicuculline (10 μM) was always added to block the inhibitory postsynaptic currents.

Ca^{2+} imaging in slice preparations

For intracellular Ca^{2+} imaging in PCs, a Ca^{2+} -sensitive dye, Oregon Green 488 BAPTA-1 (100 μM), was introduced into PCs through the patch pipette, and the concentration of EGTA in the pipette solution was decreased to 0.5 mM. Five-to-nine sequential confocal images (excitation at 488 nm), obtained at 3–4 μm z-axis intervals, were acquired every 0.8 s using an upright microscope (BX51WI; Olympus) equipped with a confocal scanning unit and an argon laser (FV300; Olympus), and projected onto a plane to obtain dendrite images at 10 or 5-s intervals.

Electrophysiological measurements

For focal stimulation of PFs, a stimulation pipette (tip diameter, 5–10 μm) was filled with standard bathing solution and used to apply square pulses (0.1 ms in duration, 0–20 V in amplitude) to the molecular layer, specifically in the middle portion of the molecular layer approximately one-third of the distance below the pial surface. The intensity of each stimulus was adjusted to evoke PF-EPSCs with an amplitude of 60–120 pA. The ionic current was recorded from PCs using a patch-clamp amplifier (EPC-9, HEKA, Lambrecht/Pfalz, Germany) at a holding potential of -90 or -80 mV, after compensating for the liquid junction potential. The signals were filtered at 2 kHz and digitized at 20 kHz.

Expression of exogenous RyR1, RyR2 and RyR3 in HEK293 cells

Full-length RyR1 cDNA (Takeshima *et al*, 1989) was subcloned into the multiple cloning sites (MCS) of the pcDNA/FRT/TO expression vector (Invitrogen, Carlsbad, CA, USA) that was modified by the addition of an *NheI* site. Tetracycline-inducible stable HEK293 cell lines were generated using the FLP-In T-REx system according to the manufacturer's instructions. RyR2 cDNA (Nakai *et al*, 1990) was similarly subcloned into the pcDNA/FRT/TO vector, and stable HEK293 cell lines were obtained (Chugun *et al*, 2007). RyR3 cDNA (Chen *et al*, 1997) (a kind gift from Dr SR Chen, University of Calgary, Alberta, Canada) was similarly expressed in HEK293 cells. FLP-InTM-293 HEK293 cells were cultured on collagen-coated dishes in Dulbecco's modified Eagle's medium supplemented with 10% fetal bovine serum, penicillin (100 U/ml), streptomycin (100 U/ml) and 2 mM glutamine. HEK293 cells at passages from 10 to 20 were plated onto collagen-coated glass-bottom dishes 3 days prior to Ca^{2+} imaging. The generation of C3635A-RyR1 is described in Supplementary data.

Cerebral neuron culture

Neurons were prepared from the cerebral cortices of wild-type or *Ryr1*^{-/-} mice fetuses (embryonic day 16 (E16) or E19) based on a modification of a previously described procedure (Kanemaru *et al*, 2007). Briefly, minced cerebral cortices were treated with 2.5% trypsin (Invitrogen) and 0.1% DNase I (Sigma-Aldrich, St Louis, MO, USA) in Ca^{2+} /Mg²⁺-free phosphate-buffered saline (PBS) for 3 min at room temperature. Cells were washed with Neurobasal-A medium (Invitrogen) supplemented with 5% fetal calf serum, penicillin (100 U/ml), streptomycin (100 U/ml) and 2 mM L-glutamine (Sigma-Aldrich) and dissociated by triturating with a fire-polished Pasteur pipette in Ca^{2+} /Mg²⁺-free PBS containing 0.05% DNase I and 0.03% trypsin inhibitor (Sigma-Aldrich). Dispersed cells were plated at 5.0 – 9.0×10^4 cells/cm² on glass coverslips that had been coated with poly-L-lysine (Sigma-Aldrich) and mouse laminin (Invitrogen). Cells were then cultured at 37°C in Neurobasal-A (Invitrogen) with B-27 supplement (Invitrogen), penicillin (100 U/ml), streptomycin (100 U/ml) and 2 mM L-glutamine under a humidified atmosphere containing 5% CO_2 . Culture medium contained 5% fetal calf serum for the first day after plating. The medium was then changed every 2 days by replacing half of the old medium with fresh medium. Cells cultured for 5–20 days were

plated onto poly-L-lysine- and laminin-coated glass coverslips 7–15 days prior to Ca²⁺ imaging. Immediately before Ca²⁺ imaging in cultured neurons, CaCl₂ in physiological salt solution (PSS) was replaced with equimolar MgCl₂ to inhibit spontaneous activity.

Ca²⁺ imaging in cultured cells

Cells were loaded at room temperature with 4 μM fura-2 AM in PSS (in mM) containing: 150 NaCl, 4 KCl, 2 CaCl₂, 1 MgCl₂, 5.6 glucose and 10 HEPES at pH 7.4. Fluorescence images were acquired at >420 nm using an inverted microscope equipped with a cooled CCD camera at a rate of one frame every 1 or 2 s. Excitation wavelengths were 345 and 380 nm. Ca²⁺ imaging experiments were conducted at room temperature, with the exception of the experiments conducted with dantrolene (35 ± 1°C). Image analyses were carried out using IPLab software (BD Biosciences Bioimaging, Rockville, MD, USA). Regions of interest (ROIs) corresponding to individual cells were selected and the mean fluorescence intensity (*F*) of each ROI minus the background intensity was calculated for each frame. We used the *F*₃₄₅/*F*₃₈₀ ratio (the value of *F* at an excitation wavelength of 345 nm divided by the value of *F* at an excitation wavelength of 380 nm) to estimate [Ca²⁺]_i, as described elsewhere (Grynkiewicz *et al*, 1985). The *K*_d (239 nM) for Ca²⁺ was determined via *in vitro* calibration of fura-2 fluorescence.

Analyses of NO-induced neuronal cell death

Primary cultured neurons were exposed to 500 μM NOC12 or vehicle, with or without 10 μM dantrolene, and cultured at 37°C. After 16 h, primary cultures were stained with 0.2 μM calcein-AM, 1 μM propidium iodide (PI) and 0.4 μM Hoechst 33342 for 10 min at room temperature. Fluorescence images were obtained at >420 nm (excitation at 350 nm) for Hoechst 33342, 515–550 nm (excitation at 480 nm) for calcein and >600 nm (excitation at 540 nm) for PI using an inverted microscope (IX70; Olympus) equipped with a ×40 (N.A. = 0.7) or ×10 (N.A. = 0.4) objective and a CCD camera. Cell death was expressed as the number of PI-positive cells divided by the number of total cells (Hoechst 33342-positive cells). High-content single-cell image analyses were undertaken using CellProfiler (Carpenter *et al*, 2006).

Biotin-switch method

S-nitrosylation of RyR1 in HEK293 cells and in cerebellar slice preparations was detected via the biotin-switch method (Jaffrey and Snyder, 2001; Ckless *et al*, 2004). This method utilizes a S-nitrosylated protein detection assay kit (Cayman Chemical, Ann Arbor, MI, USA) with some modifications, as described in Supplementary data.

MCAO model

Male 8- to 12-week-old *Nos1*^{-/-} mice and their wild-type littermates weighing 20–30 g at the time of surgery were used. Anaesthesia was

maintained during surgery with 1.5% isoflurane in a 30% O₂/70% N₂O gas mixture. Rectal and occipitocervical muscular temperatures were maintained at 37 ± 0.3°C using a heating blanket and lamp. After recovery from anaesthesia, mice were placed in an incubator at 33°C and 50% humidity to prevent hypothermia, and provided with food and water *ad libitum*. The methodology for generating the MCAO mouse model has been described previously (Chen *et al*, 2008), and is briefly described in the Supplementary data.

Determination of the infarct volume

After 24 h of reperfusion, mice were deeply anaesthetized and intracardially perfused with heparinized saline. Brains were extracted and 2-mm coronal sections were cut. Individual sections were incubated for 20 min in 2% triphenyltetrazolium chloride (TTC) in PBS at 37°C. The TTC was drained and slices were placed in 10% formalin for 30 min. Images of the slices were acquired using a digital camera. Infarct volume was calculated by two members blinded to the study protocol using the Leach correction (Leach *et al*, 1993):

$$[\text{Lesion area of each section}] = [\text{Ipsilateral lesion area}] \times \left(\frac{[\text{Contralateral hemisphere area}]}{[\text{Ipsilateral hemisphere area}]} \right)$$

Lesion volume was calculated as the sum of the lesioned areas in all five sections and multiplied by slice thickness (2 mm).

Supplementary data

Supplementary data are available at *The EMBO Journal* Online (<http://www.embojournal.org>).

Acknowledgements

This work was supported by a Grant-in-Aid for Scientific Research and a Global COE Program entitled 'Integrative Life Science Based on the Study of Biosignaling Mechanisms' from MEXT (Japan), as well as grants from the Uehara Memorial Foundation, Takeda Science Foundation, Mochida Memorial Foundation, and the Suzuken Memorial Foundation.

Author contributions: SK, TY and MI designed the research; SK, TY, YC, AI, TM, HO and HT carried out the experiments; NK, OS, MW, NM, KO, TS and NS provided new experimental tools; SK, TY, YC, AI, TM and MI analysed the data; SK and MI wrote the manuscript; and MI supervised the study.

Conflict of interest

The authors declare that they have no conflict of interest.

References

- Aghdasi B, Reid MB, Hamilton SL (1997) Nitric oxide protects the skeletal muscle Ca²⁺ release channel from oxidation induced activation. *J Biochem* **272**: 25462–25467
- Bellinger AM, Reiken S, Carlson C, Mongillo M, Liu X, Rothman L, Matecki S, Lacampagne A, Marks AR (2009) Hypernitrosylated ryanodine receptor calcium release channels are leaky in dystrophic muscle. *Nat Med* **15**: 325–330
- Berridge MJ, Lipp P, Bootman MD (2000) The versatility and universality of calcium signalling. *Nat Rev Mol Cell Biol* **1**: 11–21
- Bredt DS, Glatt CE, Hwang PM, Fotuhi M, Dawson TM, Snyder SH (1991) Nitric oxide synthase protein and mRNA are discretely localized in neuronal populations of the mammalian CNS together with NADPH diaphorase. *Neuron* **7**: 615–624
- Bredt DS, Snyder SH (1994) Nitric oxide: a physiologic messenger molecule. *Annu Rev Biochem* **63**: 175–195
- Burgoyne JR, Eaton P (2010) A rapid approach for the detection, quantification, and discovery of novel sulfenic acid or S-nitrosothiol modified proteins using a biotin-switch method. *Method Enzymol* **473**: 281–303
- Carpenter AE, Jones TR, Lamprecht MR, Clarke C, Kang IH, Friman O, Guertin DA, Chang JH, Lindquist RA, Moffat J, Golland P, Sabatini DM (2006) CellProfiler: image analysis software for identifying and quantifying cell phenotypes. *Genome Biol* **7**: R100
- Chadderton P, Margrie TW, Hausser M (2004) Integration of quanta in cerebellar granule cells during sensory processing. *Nature* **428**: 856–860
- Chen SR, Li X, Ebisawa K, Zhang L (1997) Functional characterization of the recombinant type 3 Ca²⁺ release channel (ryanodine receptor) expressed in HEK293 cells. *J Biol Chem* **272**: 24234–24246
- Chen Y, Ito A, Takai K, Saito N (2008) Blocking pterygopalatine arterial blood flow decreases infarct volume variability in a mouse model of intraluminal suture middle cerebral artery occlusion. *J Neurosci Meth* **174**: 18–24
- Chugun A, Sato O, Takeshima H, Ogawa Y (2007) Mg²⁺ activates the ryanodine receptor type 2 (RyR2) at intermediate Ca²⁺ concentrations. *Am J Physiol Cell Physiol* **292**: C535–C544
- Ckless K, Reynaert NL, Taatjes DJ, Lounsbury KM, van der Vliet A, Janssen-Heininger Y (2004) *In situ* detection and visualization of S-nitrosylated proteins following chemical derivatization: identification of Ran GTPase as a target for S-nitrosylation. *Nitric Oxide* **11**: 216–227

- Coesmans M, Weber JT, De Zeeuw CI, Hansel C (2004) Bidirectional parallel fiber plasticity in the cerebellum under climbing fiber control. *Neuron* **44**: 691–700
- Durham WJ, Aracena-Parks P, Long C, Rossi AE, Goonasekera SA, Boncompagni S, Galvan DL, Gilman CP, Baker MR, Shirokova N, Protasi F, Dirksen R, Hamilton SL (2008) RyR1 S-nitrosylation underlies environmental heat stroke and sudden death in Y522S RyR1 knockin mice. *Cell* **133**: 53–65
- Edwards FA, Konnerth A, Sakmann B, Takahashi T (1989) A thin slice preparation for patch clamp recordings from neurones of the mammalian central nervous system. *Pflügers Arch* **414**: 600–612
- Endo M (2009) Calcium-induced calcium release in skeletal muscle. *Physiol Rev* **89**: 1153–1176
- Eu JP, Hare JM, Hess DT, Skaf M, Sun J, Cardenas-Navina I, Sun QA, Dewhirst M, Meissner G, Stamler JS (2003) Concerted regulation of skeletal muscle contractility by oxygen tension and endogenous nitric oxide. *Proc Natl Acad Sci USA* **100**: 15229–15234
- Eu JP, Sun J, Xu L, Stamler JS, Meissner G (2000) The skeletal muscle calcium release channel: coupled O₂ sensor and NO signaling functions. *Cell* **102**: 499–509
- Faas GC, Raghavachari S, Lisman JE, Mody I (2011) Calmodulin as a direct detector of Ca²⁺ signals. *Nat Neurosci* **14**: 301–304
- Furuichi T, Furutama D, Hakamata Y, Nakai J, Takeshima H, Mikoshiba K (1994) Multiple types of ryanodine receptor/Ca²⁺ release channels are differentially expressed in rabbit brain. *J Neurosci* **14**: 4794–4805
- Giannini G, Conti A, Mammarella S, Scrobogna M, Sorrentino V (1995) The ryanodine receptor/calcium channel genes are widely and differentially expressed in murine brain and peripheral tissues. *J Cell Biol* **128**: 893–904
- Grynkiewicz G, Poenie M, Tsien R (1985) A new generation of Ca²⁺ indicators with greatly improved fluorescence properties. *J Biol Chem* **260**: 3440–3450
- Hess DT, Matsumoto A, Kim SO, Marshall HE, Stamler JS (2005) Protein S-nitrosylation: purview and parameters. *Nat Rev Mol Cell Biol* **6**: 150–166
- Huang PL, Dawson TM, Brecht DS, Snyder SH, Fishman MC (1993) Targeted disruption of the neuronal nitric oxide synthase gene. *Cell* **75**: 1273–1286
- Huang Y, Man HY, Sekine-Aizawa Y, Han Y, Juluri K, Luo H, Cheah J, Lowenstein C, Huganir RL, Snyder SH (2005) S-nitrosylation of N-ethylmaleimide sensitive factor mediates surface expression of AMPA receptors. *Neuron* **46**: 533–540
- Huang Z, Huang PL, Panahian N, Dalkara T, Fishman MC, Moskowitz MA (1994) Effects of cerebral ischemia in mice deficient in neuronal nitric oxide synthase. *Science* **265**: 1883–1885
- Iadecola C (1997) Bright and dark sides of nitric oxide in ischemic brain injury. *Trends Neurosci* **20**: 132–139
- Ito M (2002) The molecular organization of cerebellar long-term depression. *Nat Rev Neurosci* **3**: 896–902
- Jaffrey SR, Erdjument-Bromage H, Ferris CD, Tempst P, Snyder SH (2001) Protein S-nitrosylation: a physiological signal for neuronal nitric oxide. *Nature Cell Biol* **3**: 193–197
- Jaffrey SR, Snyder SH (2001) The biotin switch method for the detection of S-nitrosylated proteins. *Sci STKE* **2001**: PL1
- Kakegawa W, Yuzaki M (2005) A mechanism underlying AMPA receptor trafficking during cerebellar long-term potentiation. *Proc Natl Acad Sci USA* **102**: 17846–17851
- Kakizawa S, Miyazaki T, Yanagihara D, Iino M, Watanabe M, Kano M (2005) Maintenance of presynaptic function by AMPA receptor-mediated excitatory postsynaptic activity in adult brain. *Proc Natl Acad Sci USA* **102**: 19180–19185
- Kakizawa S, Yamasaki M, Watanabe M, Kano M (2000) Critical period for activity-dependent synapse elimination in developing cerebellum. *J Neurosci* **20**: 4954–4961
- Kanamaru K, Okubo Y, Hirose K, Iino M (2007) Regulation of neurite growth by spontaneous Ca²⁺ oscillations in astrocytes. *J Neurosci* **27**: 8957–8966
- Kano M, Garaschuk O, Verkhratsky A, Konnerth A (1995) Ryanodine receptor-mediated intracellular calcium release in rat cerebellar Purkinje neurons. *J Physiol* **487**: 1–16
- Kettlun C, Gonzalez A, Rios E, Fill M (2003) Unitary Ca²⁺ current through mammalian cardiac and amphibian skeletal muscle ryanodine receptor Channels under near-physiological ionic conditions. *J General Physiol* **122**: 407–417
- Kluge I, Gutteck-Amsler U, Zollinger M, Do KQ (1997) S-nitrosoglutathione in rat cerebellum: identification and quantification by liquid chromatography-mass spectrometry. *J Neurochem* **69**: 2599–2607
- Leach MJ, Swan JH, Eisenthal D, Dopson M, Nobbs M (1993) BW619C89, a glutamate release inhibitor, protects against focal cerebral ischemic damage. *Stroke* **24**: 1063–1067
- Lev-Ram V, Makings LR, Keitz PF, Kao JP, Tsien RY (1995) Long-term depression in cerebellar Purkinje neurons results from coincidence of nitric oxide and depolarization-induced Ca²⁺ transients. *Neuron* **15**: 407–415
- Lev-Ram V, Mehta SB, Kleinfeld D, Tsien RY (2003) Reversing cerebellar long-term depression. *Proc Natl Acad Sci USA* **100**: 15989–15993
- Lev-Ram V, Wong ST, Storm DR, Tsien RY (2002) A new form of cerebellar long-term potentiation is postsynaptic and depends on nitric oxide but not cAMP. *Proc Natl Acad Sci USA* **99**: 8389–8393
- Li F, Hayashi T, Jin G, Deguchi K, Nagotani S, Nagano I, Shoji M, Chan PH, Abe K (2005) The protective effect of dantrolene on ischemic neuronal cell death is associated with reduced expression of endoplasmic reticulum stress markers. *Brain Res* **1048**: 59–68
- Malinski T, Bailey F, Zhang ZG, Chopp M (1993) Nitric oxide measured by a porphyrinic microsensor in rat brain after transient middle cerebral artery occlusion. *J Cereb Blood Flow Metab* **13**: 355–358
- Moore CP, Zhang JZ, Hamilton SL (1999) A role for cysteine 3635 of RYR1 in redox modulation and calmodulin binding. *J Biol Chem* **274**: 36831–36834
- Mori F, Fukaya M, Abe H, Wakabayashi K, Watanabe M (2000) Developmental changes in expression of the three ryanodine receptor mRNAs in the mouse brain. *Neurosci Lett* **285**: 57–60
- Nakai J, Imagawa T, Hakamata Y, Shigekawa M, Takeshima H, Numa S (1990) Primary structure and functional expression from cDNA of the cardiac ryanodine receptor/calcium release channel. *FEBS Lett* **271**: 169–177
- Namiki S, Kakizawa S, Hirose K, Iino M (2005) NO signalling decodes frequency of neuronal activity and generates synapse-specific plasticity in mouse cerebellum. *J Physiol* **566**: 849–863
- Pacher P, Beckman JS, Liaudet L (2007) Nitric oxide and peroxynitrite in health and disease. *Physiol Rev* **87**: 315–424
- Peterson BZ, DeMaria CD, Adelman JP, Yue DT (1999) Calmodulin is the Ca²⁺ sensor for Ca²⁺-dependent inactivation of L-type calcium channels. *Neuron* **22**: 549–558
- Sacchetti B, Scelfo B, Tempia F, Strata P (2004) Long-term synaptic changes induced in the cerebellar cortex by fear conditioning. *Neuron* **42**: 973–982
- Sawada K, Hosoi E, Bando M, Sakata-Haga H, Lee NS, Jeong YG, Fukui Y (2008) Differential alterations in expressions of ryanodine receptor subtypes in cerebellar cortical neurons of an ataxic mutant, rolling mouse Nagoya. *Neuroscience* **152**: 609–617
- Sham JS (1997) Ca²⁺ release-induced inactivation of Ca²⁺ current in rat ventricular myocytes: evidence for local Ca²⁺ signalling. *J Physiol* **500**: 285–295
- Sun J, Xin C, Eu JP, Stamler JS, Meissner G (2001) Cysteine-3635 is responsible for skeletal muscle ryanodine receptor modulation by NO. *Proc Natl Acad Sci USA* **98**: 11158–11162
- Sun J, Yamaguchi N, Xu L, Eu JP, Stamler JS, Meissner G (2008) Regulation of the cardiac muscle ryanodine receptor by O₂ tension and S-nitrosoglutathione. *Biochemistry* **47**: 13985–13990
- Takechi H, Eilers J, Konnerth A (1998) A new class of synaptic response involving calcium release in dendritic spines. *Nature* **396**: 757–760
- Takeshima H, Iino M, Takekura H, Nishi M, Kuno J, Minowa O, Takano H, Noda T, Yamazawa T, Ikemoto T, Nishiyama N, Shimuta M, Sugitani Y, Saito I, Saito H, Endo M, Sakurai T (1994) Excitation-contraction uncoupling and muscular degeneration in mice lacking functional skeletal muscle ryanodine-receptor gene. *Nature* **369**: 556–559
- Takeshima H, Ikemoto T, Nishi M, Nishiyama N, Shimuta M, Sugitani Y, Kuno J, Saito I, Saito H, Endo M, Iino M, Noda T, Yamazawa T, Sakurai T (1996) Generation and characterization of mutant mice lacking ryanodine receptor type 3. *J Biol Chem* **271**: 19649–19652
- Takeshima H, Nishimura S, Matsumoto T, Ishida H, Kangawa K, Minamino N, Matsuo H, Ueda M, Hanaoka M, Hirose T, Numa S

- (1989) Primary structure and expression from complementary DNA of skeletal muscle ryanodine receptor. *Nature* **339**: 439–445
- Wojcikiewicz RJ (1995) Type I, II, and III inositol 1,4,5-trisphosphate receptors are unequally susceptible to down-regulation and are expressed in markedly different proportions in different cell types. *J Biol Chem* **270**: 11678–11683
- Zhao F, Li P, Chen SR, Louis CF, Fruen BR (2001) Dantrolene inhibition of ryanodine receptor Ca^{2+} release channels. Molecular mechanism and isoform selectivity. *J Biol Chem* **276**: 13810–13816
- Zühlke RD, Pitt GS, Deisseroth K, Tsien RW, Reuter H (1999) Calmodulin supports both inactivation and facilitation of L-type calcium channels. *Nature* **399**: 159–162